Measurement of water vapor adsorption isotherms in mesoporous materials using the zero length column technique

Measurement of water vapor adsorption isotherms in mesoporous materials using the zero length column technique.

*Alessio Centineo, Stefano Brandani**

School of Engineering, Institute for Materials and Processes, The University of Edinburgh, EH9 3FB, UK

Keywords: Water adsorption; Hysteresis loop; Scanning curves; Zero length column; Equilibrium

Abstract

Measurement of water adsorption isotherms is important for industrial applications and for the characterization of nanoporous materials. The zero-length column technique is used for the first time to measure the adsorption-desorption isotherm of water on a mesoporous adsorbent, SBA-15, up to 90 % relative humidity at 298 K. The technique showed two key advantages; a) The experimental flexibility for the measurement of continuous adsorption-desorption isotherms characterized by complex shapes and hysteresis loops; b) The possibility to measure a complete set of adsorption-desorption isotherms and scanning curves in few days compared to several weeks needed with traditional gravimetric techniques. The adsorption isotherm measured was compared and validated against isotherms measured on a commercial gravimetric system designed for water vapor adsorption. For the system considered, the adsorption and desorption branches are very steep, and the zero-length column technique is shown to allow setting easily the starting point of the scanning curves.

1. Introduction

The commercial and industrial applications which justify the growing interest in water vapor adsorption are numerous including gas drying (Ahn and Lee, 2004, 2003), food conservation (Qiu et al., 2019), storage of pharmaceuticals (Waterman and Macdonald, 2010), construction materials (Canivet et al., 2014), adsorption refrigeration cycles (Ruzhu Wang; Liwei Wang; Jingyi Wu, 2014) and, more recently, characterization of porous materials (Cychosz et al., 2017; Nguyen et al., 2014; Thommes et al., 2013, 2011; Velasco et al., 2016).

The utilization of water adsorption for the structural characterization of porous solids is due to its peculiar characteristics as adsorptive. Water vapor can specifically interact with the chemical groups on the surface of the solid adsorbents. In addition, water molecules are quite small, and they can easily penetrate even the tightest pores. These aspects allow water to be exploited as a probe molecule for surface chemistry investigations as well as for pore structure analysis. It can, therefore, be considered as a characterization method supplementary to the traditional methods operated with nitrogen, argon and carbon dioxide (Thommes et al., 2015, 2011). In addition, compared to the techniques based on nitrogen and argon adsorption at cryogenic conditions, water adsorption experiments can be performed at room temperature. To appreciate the potential advantages in using water for pore structural characterization, one might consider a typical water adsorption isotherm on a microporous carbon material (Thommes et al., 2012). Either nitrogen or argon, at their respective saturation temperatures, show a type I isotherm. Water, instead, shows a type IV isotherm with a relevant hysteresis loop due to the different adsorption-desorption mechanisms and to the capillary condensation phenomena (Sarkisov et al., 2017; Thommes et al.,

2012). The option to have two distinct branches potentially offers elements for a more accurate characterization of the pore structure. However, a more complex understanding and modeling of the phase behavior of water on a molecular scale is needed for an accurate evaluation, not only of the surface chemistry but also of the pores dimension and structure (Sarkisov et al., 2017).

Water vapor adsorption isotherms have traditionally been measured using either gravimetric or volumetric techniques (Baker and Sing, 1976; Naono et al., 1980; Rajniak and Yang, 1993; Sarkisov et al., 2017; Velasco et al., 2016). The easiest and cheapest method consists in measuring the mass change of a solid adsorbent when exposed to a gas phase in equilibrium with an over-saturated salt solution (Young, 2007). However, such a method is extremely time consuming and the accuracy of the experimental data can be quite poor. Commercial gravimetric instruments are typically dynamic sorption systems in which a humid stream and a dry stream are continuously mixed and sent inside the weighing chamber of the instrument. Such instruments are very accurate in a wide range of relative humidity but rather expensive. However, they suffer a lack of accuracy of the humidity detectors at very low concentrations and, therefore, it is generally not possible to evaluate correctly the Henry's law constant. Commercial volumetric instruments are very accurate and comparable in price to the gravimetric ones. These instruments are reasonably faster than the gravimetric ones, as the experiments are performed without the use of a carrier gas. Moreover, they also allow the accurate measurement of the equilibrium isotherm in the entire concentration range, Henry's law constant included, provided that water adsorption on the surfaces of the instruments is minimized. All the techniques mentioned so far can typically be considered as the most common ways to measure adsorption-desorption equilibrium isotherms on solid adsorbents. These techniques operate in a discontinuous mode, measuring a single point on the isotherm at each step. The partial pressure of the adsorptive is adjusted according to a stepwise ramp and the

uptake of adsorbate into the solid is measured for each step. This way of operating is time-consuming if accurate measurements are to be performed. Moreover, the equilibration time and/or the amount of gas dosed for each single concentration step cannot be accurately decided *a priori* and some trial runs are needed to optimize the experimental parameters. Each trial run on a gravimetric or volumetric technique can take several days. This aspect is particularly relevant for solids characterized by almost vertical adsorption or desorption branches. For these solids, the capillary condensation/evaporation branches extend over an extremely small pressure range. The measurement of the scanning curves is, therefore, not trivial as the starting points lie on a highly tight region of the isotherm. In this particular case, extremely stable concentrations of the gas phase are needed in the gravimetric technique, meanwhile, accurate values of dosed volumes are required in the volumetric techniques.

Chromatographic techniques, such as the Zero Length Column (ZLC), can be tailored and used for more rapid measurements of continuous adsorption-desorption isotherms (Brandani and Ruthven, 2003; Brandani et al., 2003). The ZLC was initially introduced and developed as a fast and reliable chromatographic method for diffusion measurements of adsorptives in microporous solids (Brandani and Ruthven, 1996a; Eic and Ruthven, 1988). The main assumptions made for the formulation of the original model are perfectly-mixed gas phase, linear equilibrium isotherm, monodispersed and microcrystalline solid adsorbent, intracrystalline or microporous diffusion mechanism, constant outlet flowrate equal to the carrier flowrate, negligible thermal effects, and negligible pressure drops. In the following years, the original model has been extended to consider the non-linearity of the adsorption isotherm (Brandani, 1998; Brandani et al., 2000), biporous adsorbents (Brandani, 1996), solids with particle or crystal size distributions (Duncan and Moller, 2002), and variable outlet flowrate (Brandani, 2005; Wang et al., 2011). Until now the technique

89 has been extensively and almost exclusively adopted for kinetic measurements. However, a ZLC
90 can work both under kinetic control conditions and under dynamic-equilibrium control conditions.
91 Therefore, the technique permits one to measure either mass transfer coefficients or adsorption-
92 desorption isotherms. The variable which is experimentally used to achieve the transition from
93 dynamic-equilibrium control to kinetic control is the carrier gas flowrate. A simple graphical check
94 can assess whether the system is under equilibrium or kinetic control conditions (Brandani, 2016;
95 Mangano et al., 2013).
96 The ZLC technique has previously been modeled and tested for the measurement of the adsorption
97 isotherms for single and multicomponent systems (Brandani et al., 2003; Brandani and Ruthven,
98 2003). Several adsorptives on different microporous solids were tested. Both linear and type I
99 adsorption isotherms were measured. The adsorption isotherm can be computed from the
100 experimental concentration curves in two different ways. The easiest way for single adsorbates
101 consists in integrating the overall mass balance in the column using the experimental concentration
102 signal at the outlet of the column (Brandani et al., 2003). The average amount adsorbed is directly
103 obtained as a function of the gas phase concentration. This method is the most recommended since
104 it provides the adsorption isotherm from a simple and robust integration of the experimental
105 concentration signal at the outlet of the column. It is also useful when the shape of the isotherm is
106 not known *a priori*. The alternative method is based on the simulation and best-correlation of the
107 ZLC response curves (Friedrich et al., 2015). In such a case, a model for the adsorption equilibrium
108 isotherm and a model for the mass transfer kinetics are needed. The system of differential equations
109 given by the overall mass balance in the system and the mass balance in the solid is to be solved
110 to correlate the gas phase concentration-response curves. Under equilibrium control conditions,
111 the shape of the simulated response curves will only depend on the adsorption isotherm parameters.

Therefore, the isotherm parameters can be computed from the best-correlation of the experimental curves.

The use of the ZLC technique for the measurement of adsorption isotherms has been demonstrated only for type I isotherms and has been validated and shown to be in good agreement with data from gravimetric or volumetric systems (Brandani et al., 2003). In addition, the experiments conducted with the ZLC system are much faster given that a complete equilibrium isotherm could be measured in few minutes (Brandani et al., 2003). The ZLC technique is, therefore, a potentially useful approach for the very time-consuming measurement of water adsorption isotherms in mesoporous materials.

In this contribution, the use of the ZLC technique has been extended to the measurement of continuous adsorption-desorption type-IV isotherms for water vapor on SBA-15. The theoretical basis with the underlying assumptions that allow to use the ZLC system is discussed in order to establish the experimental checks that must be performed. The experimental procedure will be presented with particular attention to the modifications of a traditional ZLC system for adsorption measurements of highly concentrated vapors and the experimental results are validated with independent measurements on a gravimetric system that include desorption and adsorption scanning curves.

2. ZLC equilibrium theory

The main assumption used in modelling the ZLC (Zero Length Column) technique is to consider the length of the packed bed small enough to allow a negligible gradient of the gas phase concentration along the column (Aris, 1991; Eic and Ruthven, 1988). In such a scenario, the column can be considered as a perfectly mixed tank and the concentration is assumed to be the

same in each point of the gas phase inside the bed. The thermal effects and the pressure drop in the column are practically negligible. Under these assumptions, the overall mass balance on the adsorptive and on the adsorbed phase inside the column reduces to a quite simple form that can be expressed as (Brandani et al., 2003; Brandani and Ruthven, 1996a):

$$V_s \frac{d\bar{q}}{dt} + V_f \frac{dc}{dt} = F_{in} c_{in} - F_{out} c \quad (1)$$

Where $\bar{q}$ is the average concentration in the solid; c is the vapor phase concentration inside the column; c_{in} is the vapor phase concentrations at the inlet of the column; V_s is the solid adsorbent volume in the column; V_f is the gas phase volume in the column; F_{in} and F_{out} are respectively the volumetric flowrate at the inlet and at the outlet of the column; and t is time.

The ZLC can work either under equilibrium or kinetic control conditions. The ZLC is a dynamic measurement technique in which the gas and the adsorbed phase concentrations are continuously changing during the experiment. In this scenario, the dynamic equilibrium measurements are to be interpreted as a series of infinitesimal equilibrium steps. To ensure that the adsorbed phase average concentration is at equilibrium with the gas phase concentration at any time, at least two experiments at different flowrate must be performed (Brandani, 2016). If the experimental curves measured at different flowrates overlap on a c vs $F_{out}t$ plot (*Ft-plot*), the amount adsorbed will only depend on the amount of gas passed through the column, and the system can be considered under equilibrium control conditions.

Eq. (1) can be integrated with respect to time:

$$V_s[\bar{q}(t) - \bar{q}(0)] + V_f[c(t) - c(0)] = \int_0^t F_{in} c_{in} dt - \int_0^t F_{out} c(t) dt \quad (2)$$

In an adsorption experiment: $\bar{q}(0) = 0$; $c(0) = 0$; and $c_{in} = c_0$ is set, while $c(t)$ is measured. F_{in} is also assigned while F_{out} can either be measured or can be approximated to high accuracy from

the measured concentration of the adsorptive (Brandani et al., 2003; Malek and Farooq, 1996). V_f , the volume of the gas phase inside the column, is determined from blank experiments (Brandani et al., 2003).

In a desorption experiment: $\bar{q}(0) = q_0$; $c(0) = c_0$; and $c_{in} = 0$ is set, while $c(t)$ is measured. If the adsorption experiment is carried out to full equilibration, then (c_0, q_0) is the first point on the adsorption isotherm.

For a blank experiment, Eq. (2) simplifies to:

$$V_f[c(t) - c(0)] = \int_0^t F_{in} c_{in} dt - \int_0^t F_{out} c(t) dt \quad (3)$$

Which allows to determine the final unknown, V_f.

While more complicated expressions for the variation of flowrate with time are available (Wang et al., 2011), in the case of water isotherms, the mole fraction of the adsorptive is typically below 0.05 and without loss of accuracy it is possible to calculate the outlet flowrate from the measured concentration and the carrier gas flowrate (Brandani et al., 2003; Malek and Farooq, 1996):

$$F_{out}(t) = \frac{F_{in}(1-y_{in})}{1-y(t)} = \frac{F_{carr}}{1-\frac{c(t)}{c_T}} \quad (4)$$

Where $c_T = \frac{P}{RT}$ is the molar concentration of the gas phase having assumed ideal gas behaviour; y_{in} is the molar fraction of water vapour at the inlet of the column and $y(t)$ is the molar fraction of water vapour in the column. In applying Eq. (2) to the desorption experiments it is useful to consider that the long-time asymptotic response of a ZLC system will be a single exponential decay. In this region the flowrate will also reduce to that of the carrier gas and therefore the integration can be split into two regions. A numerical integral up to a time t_{Exp}, followed by the

analytical integral of the exponential decay $a\exp(-bt)$ (Brandani and Ruthven, 1996b), which corresponds to the Henry law region (Brandani et al., 2003):

$$\int_{t_{Exp}}^{\infty} F_{carr} a \exp(-bt)\ dt = F_{carr}\frac{a}{b}\exp\left(-bt_{Exp}\right) \quad (5)$$

Provided that the experiment is carried out under equilibrium control conditions, it is therefore straightforward to obtain the experimental adsorption isotherm from an integral of the measured signal.

2.1.ZLC response curves for different isotherms

Given that all previous measurements of adsorption isotherms have been carried out for type I isotherms, it is important to understand what differences are to be expected in the dynamic response of a ZLC system when different isotherms are considered.

Under equilibrium control conditions, $\bar{q}(t) = q_{eq}[c(t)]$ and the mass balance in the system, Eq. (1), can be expressed as:

$$\left(V_s\frac{dq_{eq}}{dc} + V_f\right)\frac{dc}{dt} = F_{in}c_{in} - F_{out}c \quad (6)$$

Where dq_{eq}/dc is the derivative of the equilibrium isotherm. By assuming different isotherms linear, Langmuir and type IV, Eq. (5) can be integrated to obtain $c(t)$ and the results can be normalised defining

$$C = c/c_0 \quad (7)$$

$$Q = q_{eq}/q_0 \quad (8)$$

$$\gamma = V_f c_0/V_s q_0 \quad (9)$$

The simulated ZLC response curves for $\gamma = 0.05$ are reported in Fig. 1 for the different isotherms.

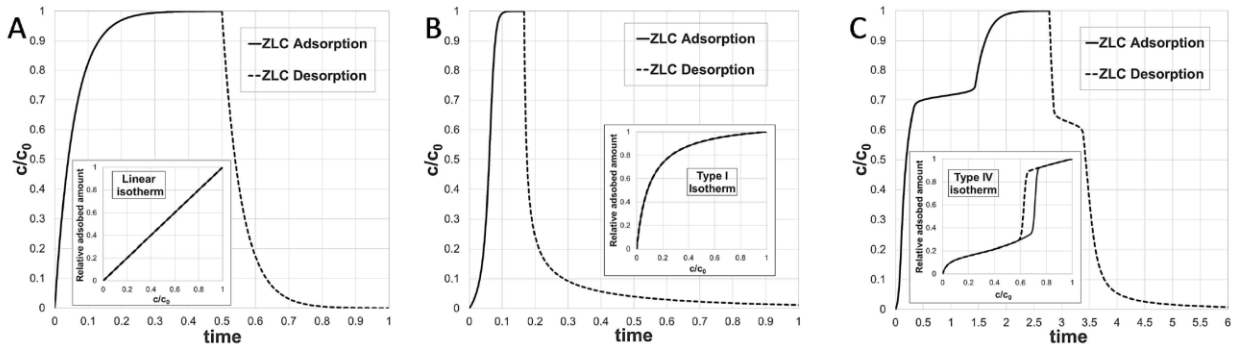

Fig. 1. (A) Adsorption-Desorption equilibrium isotherm and ZLC response curves simulated under equilibrium control conditions. Linear isotherm. (B) Adsorption-Desorption equilibrium isotherm and ZLC response curves simulated under equilibrium control conditions. Type I isotherm. (C) Adsorption-Desorption equilibrium isotherm and ZLC response curves simulated under equilibrium control conditions. Type IV isotherm.

Fig. 1a shows the characteristic symmetry of linear systems. Fig. 1b shows the typical asymmetric response of nonlinear type I systems, with the long tail in the desorption curve associated with the Henry law region. Fig. 1c shows a very interesting shape, with the condensation and evaporation branches corresponding to plateaus in the vapor phase concentration signal. It is interesting to note that what is a nearly vertical branch in a normal experiment, becomes a protracted (in time) horizontal branch in the ZLC response curve.

3. Materials and Methods

3.1.ZLC apparatus

The experimental apparatus used in this work is a purposely designed ZLC system. The simplified flowsheet of the apparatus is presented in Fig. 2. Dry nitrogen was used as carrier gas. The dry nitrogen flowrate is controlled by two 0-5 ml/min and two 0-250 ml/min SLA5850S BROOK mass

213 flow controllers. The accuracy of these mass flow controllers is ±1.0% of rate (20% - 100% FS)
214 and ±0.2% FS (below 20% FS). A 100 ml bubbler was used for the humidification of the feed line.
215 The bubbler is provided with a sparger and a demister for trapping droplets carried over by the gas
216 flow. The bubbler was immersed in a HAAKE K20 temperature-controlled bath with a DC30
217 circulator. The temperature of the bath was used to set the relative humidity of the wet nitrogen at
218 the inlet of the column. To avoid water vapor condensation, all the lines containing humid nitrogen
219 were carefully kept hot by using Omega Engineering heating ropes powered by Electrothermal
220 MC5 heating controllers. The lines were insulated with fiberglass tape. Two detectors were used
221 for the analysis of the concentration curves at the outlet of the ZLC: the first one is a quadrupole
222 Ametek Dycor Dymaxion mass spectrometer which continuously samples a flowrate of about 0.02
223 ± 0.01 ml/min of gas at the outlet of the ZLC through a silica fused capillary. The second detector
224 is a Rotronic HC2-SM humidity and temperature probe connected after the MS capillary and in
225 series with the ZLC. This probe has an accuracy of ±0.8 %rh / ±0.1 K and is the same model as
226 the humidity probe in the Aquadyne instrument. The signal of the MS was used to integrate the
227 mass balance given in Eq. (1). The signal of the humidity probe was used to measure the absolute
228 concentration of water vapor at the inlet of the column, c_0. This value is relevant for the correct
229 evaluation of the mass balance and for the position of the calculated isotherm with respect to the
230 x-axis. The relative humidity value measured by the humidity probe was approximately 95 % of
231 the equilibrium humidity value expected from the bubbler. The adsorption column was inserted
232 inside a Carbolite 3216 oven which can reach a max temperature of 350℃.

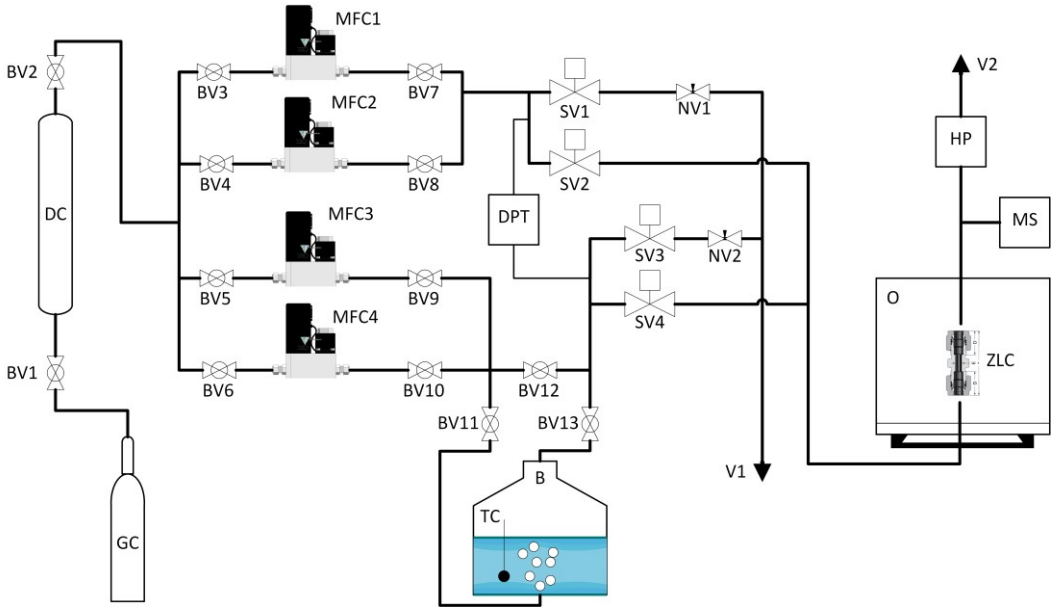

Fig. 2. Schematic flowsheet and components of the experimental ZLC system. GC carrier gas cylinder; DC drying column; BV ball valve; NV needle valve; TC water bath temperature controller; MFC mass flow controllers; B water bath; SV solenoid switching valve; V vent; O ZLC oven; ZLC zero length column; DPT differential pressure transducer; HP humidity probe; MS mass spectrometer.

The differential pressure between the adsorption and desorption lines was measured by means of a GE Unik 5000 differential pressure transducer. Two Swagelok metering valves were used at the vents to equilibrate the pressures in the two lines before switching the valves. The switch between the adsorption and desorption line was operated using four Shako solenoid valves. A commercial Quantachrome Aquadyne DVS gravimetric system was used to validate the experimental isotherms obtained with the ZLC. This gravimetric apparatus uses also a Rotronic humidity probe with the same accuracy as that on the ZLC system.

3.2.Sample preparation and loading

The details of the synthesis and preparation of the adsorbent material used in this contribution can be found in the literature (Chiang et al., 2016). A SEM image of the solid is shown in Fig. 3. The mass of solid was measured with a Mettler Toledo XS205 balance (guaranteed repeatability of ±0.05 mg) inserted inside a glove box with a continuous nitrogen flow to minimize the amount of moisture in the gas phase. Two columns were packed respectively with 3.7 mg and 1.2 mg of solid adsorbent. Prior to the first experimental run, the solid was activated *in situ* at 393 K for 3 hours under nitrogen flow. The ZLC experiments were conducted by performing several reversible adsorption-desorption cycles on the same batch. As discussed in a previous study (Centineo et al., 2019). during the first adsorption step the material changes irreversibly, trapping part of the water. Following the first experiment all the isotherms become reversible and in this study we consider only these conditions and compare the results to the gravimetric experiments from repeated exposure to water (Centineo et al., 2019).

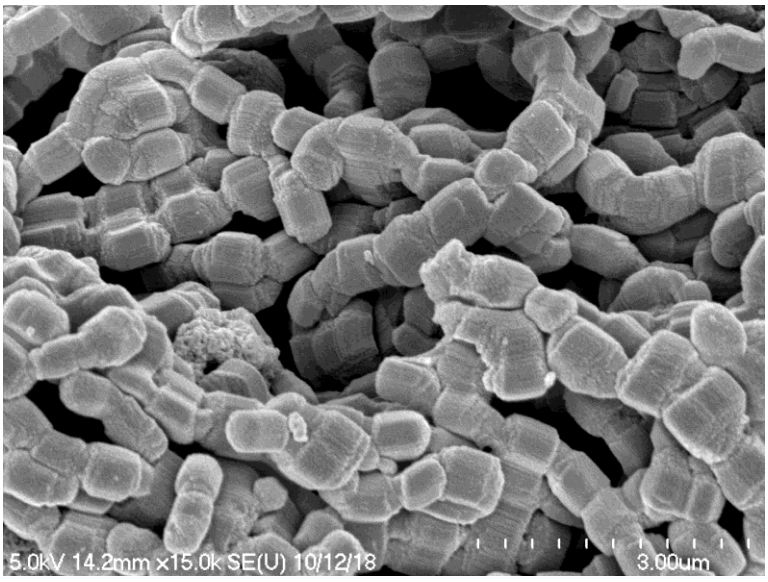

Fig. 3. SEM image of SBA-15 sample used in this study.

4. Results and Discussion

4.1.Main adsorption-desorption curves

The initial experiments were aimed to assess the control regime of the system for different desorption flowrates. Several experiments, at the same temperature and same initial concentration, were performed to find out the highest flowrate at which the system could be considered under equilibrium control conditions. As discussed beforehand, a plot of the experimental C vs Ft represents a simple and reliable graphical check for the assessment of the control regime of the system (Brandani, 2016).

The different control regimes can clearly be observed in Fig. 4 where several desorption curves measured at different flowrates are plotted on an *Ft-plot*. At the highest flowrate, the shape of the response curve is similar to that of a type-I isotherm. It is therefore essential to be able to change the flowrate until overlap of curves on the *Ft-plot* is achieved.

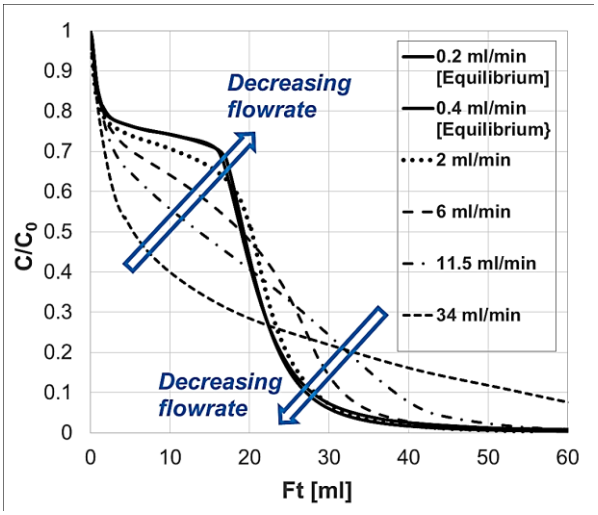

Fig. 4. Experimental *Ft-plot* for the evaluation of the control regime. Sample mass 1.2 mg. Initial relative humidity = 86 %, at 298K and atmospheric pressure.

When the flowrate is sufficiently low, the response curves approach the equilibrium regime and the effect of the shape of the isotherm becomes clearly visible. Indeed, the curves obtained at the two lowest flowrates overlap completely and, therefore, these can be considered under equilibrium control conditions and the integral can be performed to obtain the measured desorption isotherm shown in Fig. 5. It must be considered that the mass spectrometer can acquire data at high frequency and, therefore, practically continuous adsorption-desorption isotherms can be obtained. Fig. 5 is, in fact, a curve with 10^4 experimental points and the integration procedure helps also in smoothing the noise of the original signal. As this is the first time that such an isotherm is obtained from a ZLC measurement, it is worth noting that extremely low flowrates, less than 1 ml/min, are required to reach equilibrium control conditions. This implies also the need to couple the ZLC system to a mass spectrometer that has a very low inlet flowrate in the capillary. Not all commercial quadrupole mass spectrometers can be used in this configuration unless a make-up gas is used, but this then dilutes the signal.

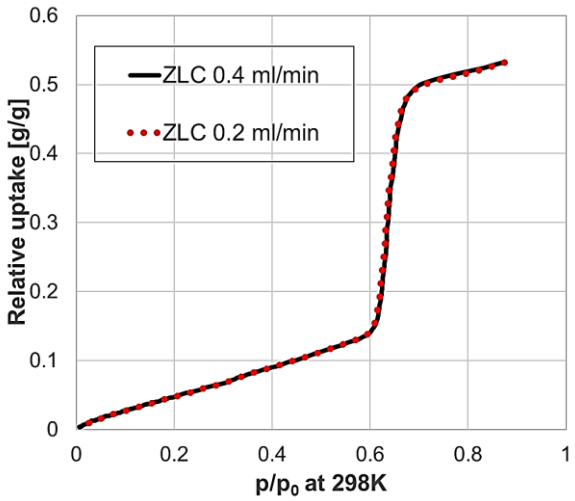

Fig. 5. Desorption isotherm calculated by using the two lowest flowrates shown in Fig. 4. Sample mass 1.2 mg. Initial relative humidity = 86 % at 298K and atmospheric pressure.

The fact that at higher flowrates the system is under kinetic control indicates that it is also possible to use the same instrument to measure kinetic properties, but the focus of this contribution is that of determining accurate equilibrium properties. It is important to note that the interpretation of kinetic experiments requires the knowledge of the derivative of the adsorption isotherm (Chmelik and Kärger, 2016; Glover et al., 2008; Hefti et al., 2015; Kärger et al., 2012; Lin et al., 1996; Ruthven, 1984) and clearly this can be estimated accurately from ZLC measurements given the large number of points available, particularly in the adsorption and desorption branches.

The blank response of the system, which is used to calculate V_f in Eq. (1), is practically negligible if compared to the desorption run (Fig. 6). Moreover, to verify the assumption of negligible thermal effects and pressure drops, the adsorption-desorption isotherm was measured with two different masses of sample showing a near-perfect reproducibility (Fig. 7).

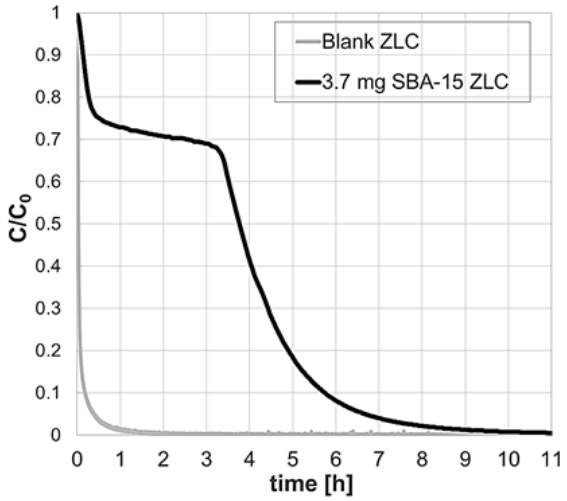

Fig. 6. Experimental response curves for the blank column and packed column. Sample mass 3.7 mg. Initial relative humidity = 86 % at 298K and atmospheric pressure.

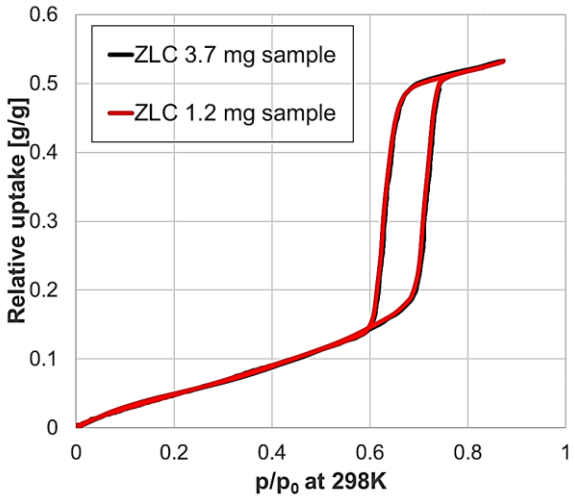

306

307 **Fig. 7.** Adsorption and desorption isotherms measured using two different sample masses. Initial
308 relative humidity = 86 % and atmospheric pressure.

309 Fig. 8 shows the continuous isotherm calculated from the ZLC signal and the equilibrium isotherm
310 measured on the gravimetric system used as reference. The excellent agreement between the two
311 isotherms measured with two independent systems validates the experimental protocols used in
312 the ZLC technique and confirms that the possible uncertainty is within 2% which corresponds
313 approximately to the size of the symbols used for the gravimetric data. The main advantage of the
314 ZLC measurement is particularly evident in the adsorption and desorption branches. It is very
315 difficult to measure several points in these regions using the gravimetric system and as a result,
316 there is a much larger uncertainty in the slope of the isotherm in these regions. Given that this is
317 where the kinetic limitations are more evident (see Fig. 4), it is also the region where an accurate
318 estimate of the derivative of the isotherm is needed for the interpretation of kinetic experiments.

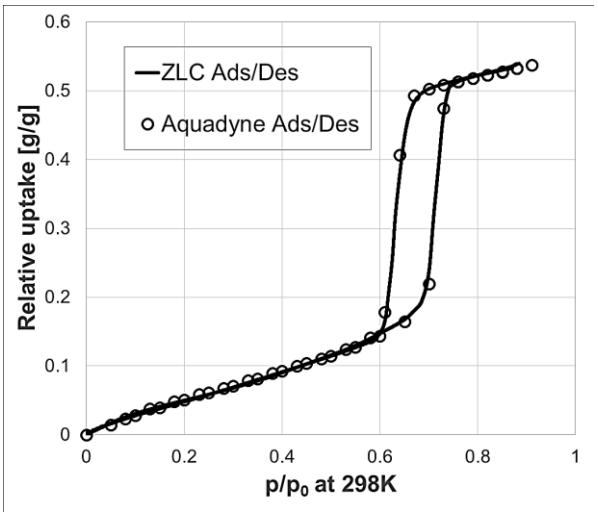

319

320 **Fig. 8.** Comparison between the isotherms measured with the ZLC system and gravimetric system.
321 ZLC sample mass 3.7 mg. Gravimetric sample mass 7 mg. Initial relative humidity = 86 % and
322 atmospheric pressure. Experimental signals are shown in Fig. 9.

323 Fig. 9 shows the second remarkable advantage of the ZLC technique. Given that the entire isotherm
324 is determined continuously, the time needed to produce the full adsorption and desorption cycle is
325 approximately 1.4 days compared to 9 days of the gravimetric experiment. In the gravimetric
326 experiment, one could reduce the time needed by reducing the number of points on the curves,
327 since the limiting process is the equilibration time of the individual points but to have a sufficiently
328 detailed isotherm one would still need several days to one week. Here clearly one can see the
329 potential of coupling a ZLC system with a gravimetric or volumetric apparatus since the ZLC can
330 provide an accurate shape of the isotherm rapidly, while the single point-based measurements can
331 provide an independent confirmation of the absolute accuracy of the ZLC results. This can be
332 important when very small sample masses are used in the ZLC measurement.

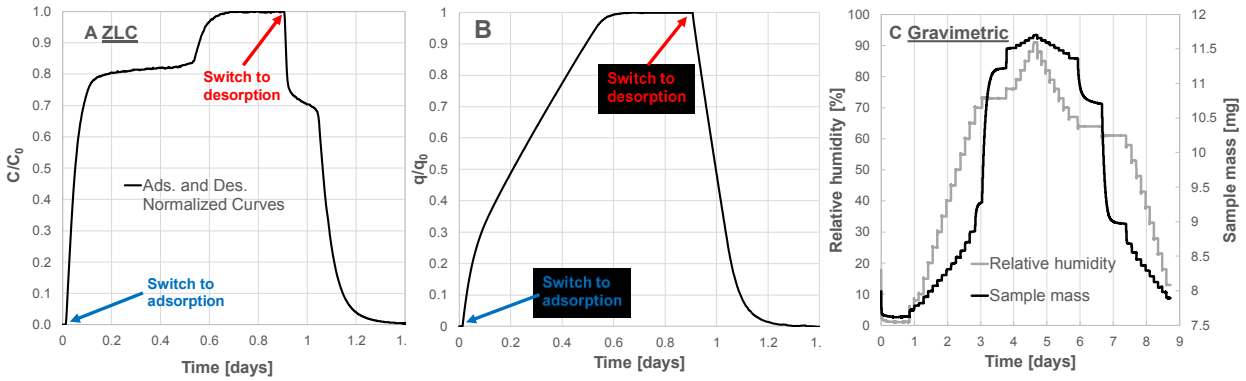

Fig. 9. (A) Experimental adsorption-desorption normalized response curves measured under equilibrium control conditions on the ZLC. (B) Adsorbed phase concentration vs time obtained from ZLC mass balance. Sample mass 3.7 mg. Highest relative humidity = 86 % at 298K and atmospheric pressure. (C) Experimental uptake curves obtained from the measurement of the equilibrium adsorption-desorption isotherm on the gravimetric system. Sample mass 7 mg.

4.2.Scanning curves

The advantages of the ZLC extend to the measurement of the scanning curves, i.e. the curves which scan the hysteresis loop from the adsorption branch to the desorption branch and *vice versa*. These curves are defined as adsorption or desorption scanning curves according to the starting point and direction along the equilibrium isotherm (Monson, 2012). The trajectory of these curves is strictly correlated to the pore structure of the solids (Cychosz et al., 2017). Scanning curves have recently gained interest as a powerful and essential tool for the systematic characterization of the inner structure of nanoporous solids (Cordero et al., 2002; Cychosz et al., 2017; Klomkliang et al., 2015, 2014; Monson, 2012; Morishige, 2017; Sarkisov et al., 2017; Tompsett et al., 2005; Zeng et al., 2016). Therefore, the possibility to measure continuous and accurate scanning curves would represent a considerable step forward in the structural characterization of porous solids.

For the efficient measurement of the scanning curves, it is important to appreciate the correlation between the shape of the signal and the isotherm. In the ZLC experiment the measured quantity is the partial pressure of water, therefore the adsorption and desorption branches result in horizontal plateaus where the isotherm is very sharp. This is clearly highlighted in Fig. 10, which shows the normalized signal vs time. Fig. 11 shows the regions corresponding to the two plateaus in the isotherm.

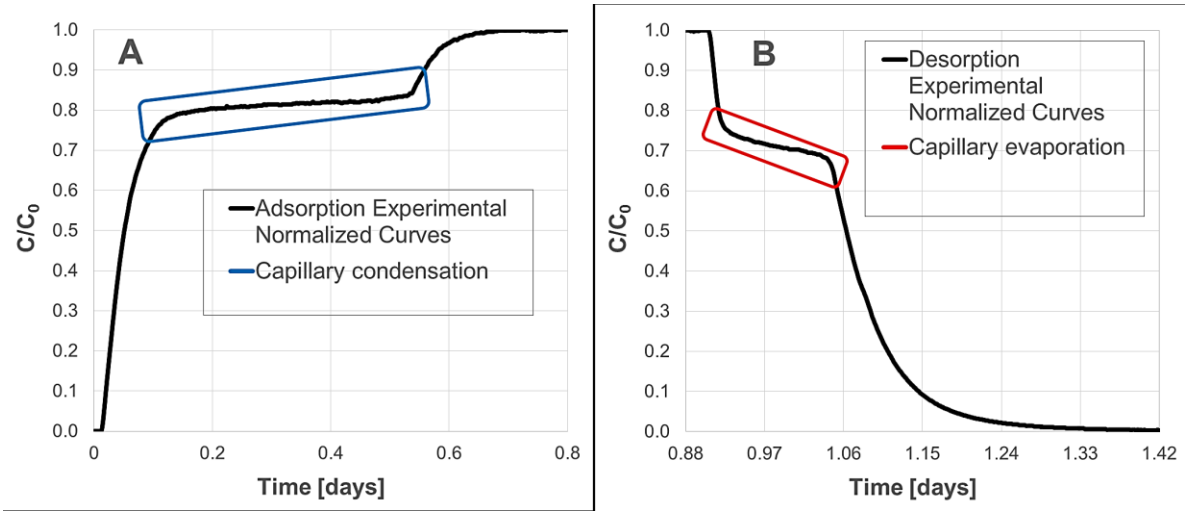

Fig. 10. Experimental normalized response curves measured under equilibrium control conditions on the ZLC at 298K and atmospheric pressure. Sample mass 3.7 mg. (A) Measurement of the main adsorption branch. Final relative humidity = 86 %. (B) Measurement of the main desorption branch. Initial relative humidity = 86 %.

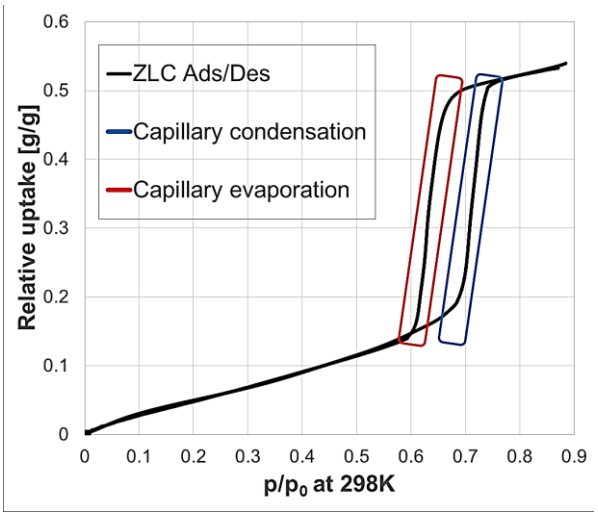

Fig. 11. Experimental adsorption-desorption isotherm calculated from the ZLC response curves shown in Fig. 10. Sample mass 3.7 mg. Highest relative humidity = 86 % at 298K and atmospheric pressure.

From Fig. 10, if the valve is switched at any time between 0.15 and 0.55 days a desorption scanning curve is obtained. Figure 9B can be used to determine the adsorbed phase concentration at the start of the scanning experiment. This should be compared to setting the partial pressure in a traditional experiment to between 70 and 73% relative humidity. Even with a very accurate control of the relative humidity, performing more than 2 scanning curves at precise locations is a challenge using a single-point based technique. On the other hand, with the ZLC one can automate the valve switching times and could generate a large number of scanning curves without difficulty. A similar analysis applies to the desorption branch, which extends between 0.9 and 1 day, i.e. more than 2 hours. This is a sufficiently broad period of time to allow for several adsorption scanning curves, considering that the valve switching time is a fraction of a second.

Just for clarity, it is important to stress that this method is based on having established the conditions for equilibrium control. Under these conditions, the adsorption or desorption experiment is run for a fixed period of time and the valve is switched while the concentrations are

within the hysteresis loop, to obtain scanning curves. Fig. 12 shows the experimental signal for desorption and adsorption scanning curves as an example of the methodology.

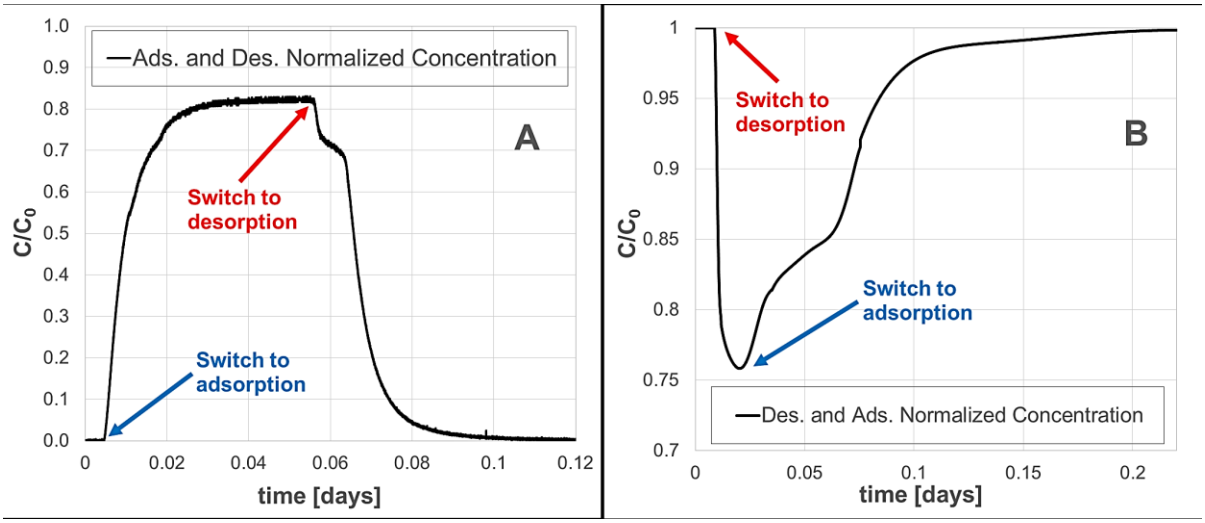

Fig. 12. Experimental adsorption-desorption normalized response curve measured under equilibrium control conditions at 298K and atmospheric pressure for sample mass 3.7 mg. (A) Measurement of the desorption scanning curve, t_{switch} = 12110 s. Initial relative humidity = 71.5 %. (B) Measurement of the adsorption scanning curve, t_{switch} = 1710 s. Initial relative humidity = 64 %.

Fig. 13 shows the full comparison of the measured scanning curves with the ZLC and the gravimetric system (under similar starting conditions). The comparisons show that again the ZLC results are validated and it is clear that the continuous scanning curves have significant detail, particularly in the way in which the curves join with the opposite branch. In addition, a traditional gravimetric instrument would approximately require between one to two months for the accurate measurement of a complete set (at least 3 different temperatures) of main adsorption/desorption curves and scanning curves. The ZLC can be used to measure the same curves with more definition in a single week.

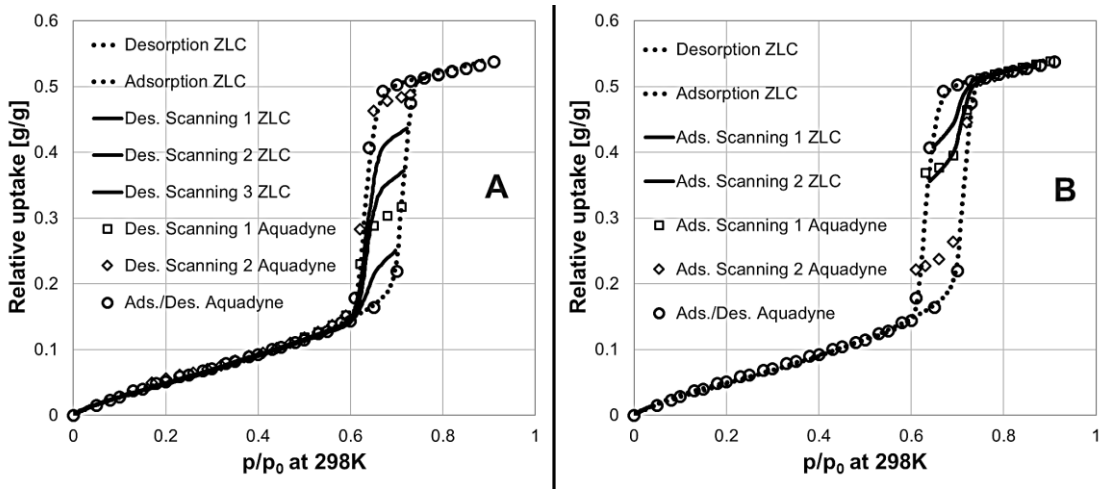

Fig. 13. (A) Desorption scanning curves measured on the ZLC system and gravimetric system. Initial relative humidity = 72.2 %, 71.5 % and, 69.7 %. ZLC sample mass 3.7 mg. Gravimetric sample mass 7 mg. (B) Adsorption scanning curves measured on the ZLC system and gravimetric system. Initial relative humidity = 64 % and, 64.8 %. ZLC sample mass 3.7 mg at 298K and atmospheric pressure. Gravimetric sample mass 7 mg.

5. Conclusions

In this contribution, the innovative and effective use of the ZLC technique for the measurement of type IV adsorption isotherms was demonstrated. The technique was able to accurately reproduce the complex shape of water vapor adsorption-desorption isotherms on SBA-15. The adsorption-desorption isotherms were obtained by means of a simple and robust integration of the ZLC response curves.

Experiments at different flowrates and with different sample masses were performed to exclude the presence of any thermal effects and pressure drops, thus, confirming the assumptions of the ZLC technique. Extremely low flowrates were required to approach the equilibrium control

411 conditions, suggesting a slow mass transport for water vapor into the solid. The blank experiment
412 permitted to exclude any condensation of water vapor in the lines as the response integral was
413 virtually negligible when compared to the column response.
414 The ZLC technique was coupled with a high-frequency sampling mass spectrometer which
415 permitted the calculation of what is essentially a continuous isotherm. This accurate determination
416 of the shape of the isotherm allows to calculate also the derivative of the isotherm, which is relevant
417 for kinetic studies.
418 The ZLC data were validated against the equilibrium isotherm measured on an independent
419 commercial gravimetric system designed for water adsorption measurements, showing excellent
420 agreement. One of the main advantages of the ZLC is that it is intrinsically faster, by up to an order
421 of magnitude, and can provide virtually continuous adsorption-desorption isotherms. For
422 isotherms characterized by almost vertical adsorption/desorption branches, as in the case of SBA-
423 15, the ZLC provides considerably more detail compared to any single-point equilibration
424 technique. Compared to traditional techniques the main disadvantage is that the isotherm is
425 obtained from the numerical integration of the concentration signal rather than being the directly
426 measured quantity.
427 The ZLC was also used to determine adsorption and desorption scanning curves. Another
428 significant advantage of the ZLC is the fact that the very narrow pressure ranges over which
429 condensation and evaporation occur become relatively long time intervals thus allowing to select
430 easily the starting points for scanning experiments. Obtaining virtually continuous scanning curves
431 provides increased detail, especially where the scanning curve re-joins the opposite branch of the
432 hysteresis loop.

433

Corresponding Author

* E-mail: s.brandani@ed.ac.uk.

ORCID

Stefano Brandani: 0000-0001-9470-6837

Funding Sources

One of the authors (A.C.) acknowledges the support received from The University of Edinburgh, PSE Ltd and the Energy Technologies Partnership who funded his PhD studentship.

Acknowledgments

SBA-15 samples were provided by Dr. Emiliano Fratini and Dr. Piero Baglioni from the University of Florence.

References

Ahn, H., Lee, C.H., 2004. Effects of capillary condensation on adsorption and thermal desorption dynamics of water in zeolite 13X and layered beds. Chem. Eng. Sci. 59, 2727–2743. https://doi.org/10.1016/j.ces.2004.04.011

Ahn, H., Lee, C.H., 2003. Adsorption dynamics of water in layered bed for air-drying TSA process. AIChE J. 49, 1601–1609. https://doi.org/10.1002/aic.690490623

Aris, R., 1991. Manners makyth modellers. Chem. Eng. Sci. 46, 1535–1544. https://doi.org/10.1016/0009-2509(91)87003-U

Baker, F.S., Sing, K.S.W., 1976. Specificity in the adsorption of nitrogen and water on hydroxylated and dehydroxylated silicas. J. Colloid Interface Sci. 55, 605–613. https://doi.org/10.1016/0021-9797(76)90071-0

Brandani, F., Ruthven, D., 2003. Measurement of Adsorption Equilibria by the Zero Length Column (ZLC) Technique Part 2: Binary Systems. Ind. Eng. Chem. Res. 42, 1462–1469. https://doi.org/10.1021/ie020573f

Brandani, F., Ruthven, D., Coe, C.G., 2003. Measurement of adsorption equilibrium by the zero length column (ZLC) technique part 1: Single-component systems. Ind. Eng. Chem. Res. 42, 1451–1461. https://doi.org/10.1021/ie020572n

Brandani, S., 2016. A Simple Graphical Check of Consistency for Zero Length Column Desorption Curves. Chem. Eng. Technol. 39, 1194–1198. https://doi.org/10.1002/ceat.201500634

Brandani, S., 2005. On the chromatographic measurement of equilibrium isotherms using large concentration steps. Adsorption 11, 231–235. https://doi.org/10.1007/s10450-005-5929-0

Brandani, S., 1998. Effects of nonlinear equilibrium on zero length column experiments. Chem. Eng. Sci. 53, 2791–2798. https://doi.org/10.1016/S0009-2509(98)00075-X

Brandani, S., 1996. Analytical solution for ZLC desorption curves with bi-porous adsorbent particles. Chem. Eng. Sci. 51, 3283–3288. https://doi.org/10.1016/0009-2509(95)00399-1

Brandani, S., Jama, M.A., Ruthven, D.M., 2000. ZLC measurements under non-linear conditions. Chem. Eng. Sci. 55, 1205–1212. https://doi.org/10.1016/S0009-2509(99)00411-X

Brandani, S., Ruthven, D.M., 1996a. Analysis of ZLC desorption curves for gaseous systems. Adsorption 2, 133–143. https://doi.org/10.1007/BF00127043

Brandani, S., Ruthven, D.M., 1996b. Moments Analysis of the Zero Length Column Method. Ind. Eng. Chem. Res. 35, 315–319. https://doi.org/10.1021/ie950287m

Canivet, J., Fateeva, A., Guo, Y., Coasne, B., Farrusseng, D., 2014. Water adsorption in MOFs: fundamentals and applications. Chem. Soc. Rev. 43, 5594–5617. https://doi.org/10.1039/C4CS00078A

Centineo, A., Nguyen, H.G.T., Espinal, L., Horn, J.C., Brandani, S., 2019. An experimental and modelling study of water vapour adsorption on SBA-15. Microporous Mesoporous Mater. 282, 53–72. https://doi.org/https://doi.org/10.1016/j.micromeso.2019.03.018

Chiang, W.S., Fratini, E., Baglioni, P., Georgi, D., Chen, J.H., Liu, Y., 2016. Methane Adsorption in Model Mesoporous Material, SBA-15, Studied by Small-Angle Neutron Scattering. J.

Phys. Chem. C 120, 4354–4363. https://doi.org/10.1021/acs.jpcc.5b10688

Chmelik, C., Kärger, J., 2016. The predictive power of classical transition state theory revealed in diffusion studies with MOF ZIF-8. Microporous Mesoporous Mater. 225, 128–132. https://doi.org/10.1016/j.micromeso.2015.11.051

Cordero, S., Rojas, F., Kornhauser, I., Domínguez, A., Vidales, A.M., López, R., Zgrablich, G., Riccardo, J.L., 2002. Pore-blocking and pore-assisting factors during capillary condensation and evaporation. Appl. Surf. Sci. 196, 224–238. https://doi.org/10.1016/S0169-4332(02)00061-2

Cychosz, K.A., Guillet-Nicolas, R., García-Martínez, J., Thommes, M., 2017. Recent advances in the textural characterization of hierarchically structured nanoporous materials. Chem. Soc. Rev. 46, 389–414. https://doi.org/10.1039/c6cs00391e

Duncan, W.L., Moller, K.P., 2002. The effect of a crystal size distribution on ZLC experiments. Chem. Eng. Sci. 57, 2641–2652. https://doi.org/10.1016/S0009-2509(02)00161-6

Eic, M., Ruthven, D.M., 1988. A new experimental technique for measurement of intracrystalline diffusivity. Zeolites 8, 40–45. https://doi.org/10.1016/S0144-2449(88)80028-9

Friedrich, D., Mangano, E., Brandani, S., 2015. Automatic estimation of kinetic and isotherm parameters from ZLC experiments. Chem. Eng. Sci. 126, 616–624. https://doi.org/10.1016/j.ces.2014.12.062

Glover, T.G., Wang, Y., Van, M.D. Le, 2008. Diffusion of condensable vapors in single adsorbent particles measured via concentration-swing frequency response. Langmuir 24, 13406–13413.

https://doi.org/10.1021/la802222r

Hefti, M., Joss, L., Marx, D., Mazzotti, M., 2015. An Experimental and Modeling Study of the Adsorption Equilibrium and Dynamics of Water Vapor on Activated Carbon. Ind. Eng. Chem. Res. 54, 12165–12176. https://doi.org/10.1021/acs.iecr.5b03445

Kärger, J., Ruthven, D.M., Theodorou, D.N., 2012. Diffusion in Nanoporous Materials. Copyright © 2012 Wiley- VCH Verlag GmbH & Co. KGaA, Weinheim, Germany. https://doi.org/10.1002/9783527651276

Klomkliang, N., Do, D.D., Nicholson, D., 2015. Hysteresis loop and scanning curves for argon adsorbed in mesopore arrays composed of two cavities and three necks. J. Phys. Chem. C 119, 9355–9363. https://doi.org/10.1021/acs.jpcc.5b01184

Klomkliang, N., Do, D.D., Nicholson, D., 2014. Hysteresis loop and scanning curves of argon adsorption in closed-end wedge pores. Langmuir 30, 12879–12887. https://doi.org/10.1021/la5035992

Lin, T.-F., Little, J.C., Nazaroff, W.W., 1996. Transport and Sorption of Organic Gases in Activated Carbon. J. Environ. Eng. 122, 169–175. https://doi.org/10.1061/(ASCE)0733-9372(1996)122:3(169)

Malek, A., Farooq, S., 1996. Effect of velocity variation on equilibrium calculations from multicomponent breakthrough experiments. Chem. Eng. Sci. 52, 443–447. https://doi.org/10.1016/S0009-2509(96)00417-4

Mangano, E., Brandani, S., Ruthven, D.M., 2013. Analysis and interpretation of zero length

column response curves. Chemie-Ingenieur-Technik 85, 1714–1718. https://doi.org/10.1002/cite.201300083

Monson, P.A., 2012. Understanding adsorption/desorption hysteresis for fluids in mesoporous materials using simple molecular models and classical density functional theory. Microporous Mesoporous Mater. 160, 47–66. https://doi.org/10.1016/j.micromeso.2012.04.043

Morishige, K., 2017. Dependent Domain Model of Cylindrical Pores. J. Phys. Chem. C 121, 5099–5107. https://doi.org/10.1021/acs.jpcc.6b12566

Naono, H., Fujiwara, R., Yagi, M., 1980. Determination of physisorbed and chemisorbed waters on silica gel and porous silica glass by means of desorption isotherms of water vapor. J. Colloid Interface Sci. 76, 74–82. https://doi.org/10.1016/0021-9797(80)90272-6

Nguyen, V.T., Horikawa, T., Do, D.D., Nicholson, D., 2014. Water as a potential molecular probe for functional groups on carbon surfaces. Carbon N. Y. 67, 72–78. https://doi.org/10.1016/j.carbon.2013.09.057

Qiu, L., Zhang, M., Tang, J., Adhikari, B., Cao, P., 2019. Innovative technologies for producing and preserving intermediate moisture foods: A review. Food Res. Int. 116, 90–102. https://doi.org/10.1016/J.FOODRES.2018.12.055

Rajniak, P., Yang, R.T., 1993. A Simple Model and Experiments for Adsorption- Desorption Hysteresis : Water Vapor on Silica Gel 39.

Ruthven, D.M., 1984. Principles of Adsorption and Adsorption Processes, Wiley-Interscience

publication. Wiley, New York.

Ruzhu Wang; Liwei Wang; Jingyi Wu, 2014. Adsorption Refrigeration Technology: Theory and Application. Copyright © 2014 John Wiley & Sons, Singapore Pte. Ltd., Singapore. https://doi.org/10.1002/9781118197448

Sarkisov, L., Centineo, A., Brandani, S., 2017. Molecular simulation and experiments of water adsorption in a high surface area activated carbon: Hysteresis, scanning curves and spatial organization of water clusters. Carbon N. Y. 118, 127–138. https://doi.org/10.1016/j.carbon.2017.03.044

Thommes, M., Cychosz, K.A., Neimark, A. V, 2012. Chapter 4 - Advanced Physical Adsorption Characterization of Nanoporous Carbons, in: Tascón, J.M.D. (Ed.), Novel Carbon Adsorbents. Elsevier, Oxford, pp. 107–145. https://doi.org/https://doi.org/10.1016/B978-0-08-097744-7.00004-1

Thommes, M., Kaneko, K., Neimark, A. V., Olivier, J.P., Rodriguez-Reinoso, F., Rouquerol, J., Sing, K.S.W., 2015. Physisorption of gases, with special reference to the evaluation of surface area and pore size distribution (IUPAC Technical Report). Pure Appl. Chem. 87, 1051–1069. https://doi.org/10.1515/pac-2014-1117

Thommes, M., Morell, J., Cychosz, K.A., Fröba, M., 2013. Combining Nitrogen, Argon, and Water Adsorption for Advanced Characterization of Ordered Mesoporous Carbons (CMKs) and Periodic Mesoporous Organosilicas (PMOs). Langmuir 29, 14893–14902. https://doi.org/10.1021/la402832b

Thommes, M., Morlay, C., Ahmad, R., Joly, J.P., 2011. Assessing surface chemistry and pore

structure of active carbons by a combination of physisorption (H2O, Ar, N2, CO2), XPS and TPD-MS. Adsorption 17, 653–661. https://doi.org/10.1007/s10450-011-9360-4

Tompsett, G.A., Krogh, L., Griffin, D.W., Conner, W.C., 2005. Hysteresis and scanning behavior of mesoporous molecular sieves. Langmuir 21, 8214–8225. https://doi.org/10.1021/la050068y

Velasco, L.F., Guillet-Nicolas, R., Dobos, G., Thommes, M., Lodewyckx, P., 2016. Towards a better understanding of water adsorption hysteresis in activated carbons by scanning isotherms. Carbon N. Y. 96, 753–758. https://doi.org/10.1016/j.carbon.2015.10.017

Wang, H., Brandani, S., Lin, G., Hu, X., 2011. Flowrate correction for the determination of isotherms and Darken thermodynamic factors from Zero Length Column (ZLC) experiments. Adsorption 17, 687–694. https://doi.org/10.1007/s10450-011-9364-0

Waterman, K.C., Macdonald, B.C., 2010. Package Selection for Moisture Protection for Solid, Oral Drug Products. J. Pharm. Sci. 99, 4437–4452. https://doi.org/10.1002/JPS.22161

Young, J.F., 2007. Humidity control in the laboratory using salt solutions—a review. J. Appl. Chem. 17, 241–245. https://doi.org/doi:10.1002/jctb.5010170901

Zeng, Y., Tan, S.J., Do, D.D., Nicholson, D., 2016. Hysteresis and scanning curves in linear arrays of mesopores with two cavities and three necks. Classification of the scanning curves. Colloids Surfaces A Physicochem. Eng. Asp. 496, 52–62. https://doi.org/10.1016/j.colsurfa.2015.08.023

Abstract Graphic

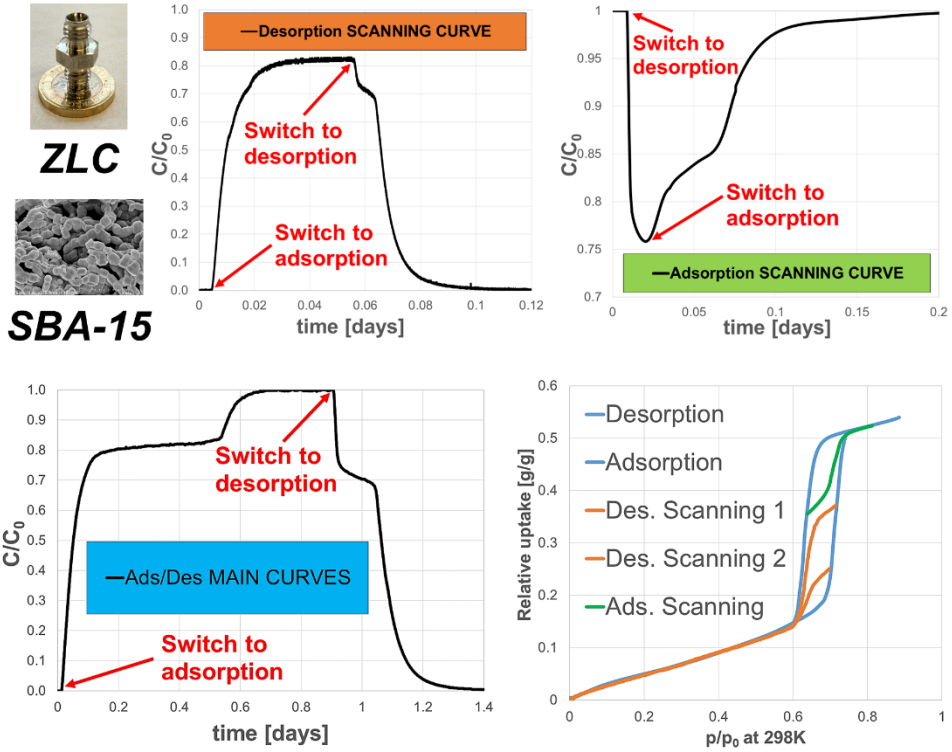

List of figures

Fig. 1. (A) Adsorption-Desorption equilibrium isotherm and ZLC response curves simulated under equilibrium control conditions. Linear isotherm. (B) Adsorption-Desorption equilibrium isotherm and ZLC response curves simulated under equilibrium control conditions. Type I isotherm. (C) Adsorption-Desorption equilibrium isotherm and ZLC response curves simulated under equilibrium control conditions. Type IV isotherm.

Fig. 2. Schematic flowsheet and components of the experimental ZLC system. GC carrier gas cylinder; DC drying column; BV ball valve; NV needle valve; TC water bath temperature controller; MFC mass flow controllers; B water bath; SV solenoid switching valve; V vent; O ZLC oven; ZLC zero length column; DPT differential pressure transducer; HP humidity probe; MS mass spectrometer.

Fig. 3. SEM image of SBA-15 sample used in this study.

Fig. 4. Experimental *Ft-plot* for the evaluation of the control regime. Sample mass 1.2 mg. Initial relative humidity = 86 %, at 298K and atmospheric pressure.

Fig. 5. Desorption isotherm calculated by using the two lowest flowrates shown in Fig. 4. Sample mass 1.2 mg. Initial relative humidity = 86 % at 298K and atmospheric pressure.

Fig. 6. Experimental response curves for the blank column and packed column. Sample mass 3.7 mg. Initial relative humidity = 86 % at 298K and atmospheric pressure.

Fig. 7. Adsorption and desorption isotherms measured using two different sample masses. Initial relative humidity = 86 % and atmospheric pressure.

Fig. 8. Comparison between the isotherms measured with the ZLC system and gravimetric system. ZLC sample mass 3.7 mg. Gravimetric sample mass 7 mg. Initial relative humidity = 86 % and atmospheric pressure. Experimental signals are shown in Fig. 9.

Fig. 9. (A) Experimental adsorption-desorption normalized response curves measured under equilibrium control conditions on the ZLC. (B) Adsorbed phase concentration vs time obtained from ZLC mass balance. Sample mass 3.7 mg. Highest relative humidity = 86 % at 298K and atmospheric pressure. (C) Experimental uptake curves obtained from the measurement of the equilibrium adsorption-desorption isotherm on the gravimetric system. Sample mass 7 mg.

Fig. 10. Experimental normalized response curves measured under equilibrium control conditions on the ZLC at 298K and atmospheric pressure. Sample mass 3.7 mg. (A) Measurement of the main adsorption branch. Final relative humidity = 86 %. (B) Measurement of the main desorption branch. Initial relative humidity = 86 %.

Fig. 11. Experimental adsorption-desorption isotherm calculated from the ZLC response curves shown in Fig. 10. Sample mass 3.7 mg. Highest relative humidity = 86 % at 298K and atmospheric pressure.

Fig. 12. Experimental adsorption-desorption normalized response curve measured under equilibrium control conditions at 298K and atmospheric pressure for sample mass 3.7 mg. (A) Measurement of the desorption scanning curve, t_{switch} = 12110 s. Initial relative humidity = 71.5 %. (B) Measurement of the adsorption scanning curve, t_{switch} = 1710 s. Initial relative humidity = 64 %.

Fig. 13. (A) Desorption scanning curves measured on the ZLC system and gravimetric system. Initial relative humidity = 72.2 %, 71.5 % and, 69.7 %. ZLC sample mass 3.7 mg. Gravimetric sample mass 7 mg. (B) Adsorption scanning curves measured on the ZLC system and gravimetric system. Initial relative humidity = 64 % and, 64.8 %. ZLC sample mass 3.7 mg at 298K and atmospheric pressure. Gravimetric sample mass 7 mg.

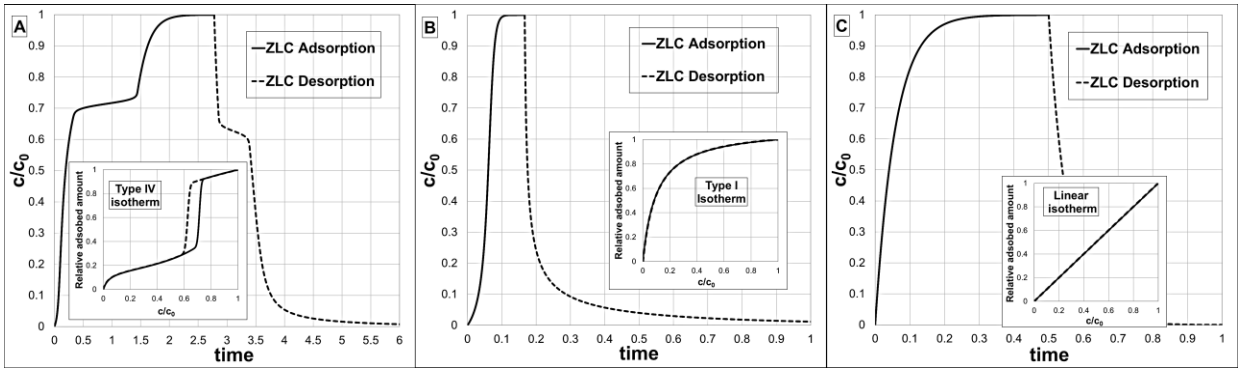

Fig. 1. (A) Adsorption-Desorption equilibrium isotherm and ZLC response curves simulated under equilibrium control conditions. Linear isotherm. (B) Adsorption-Desorption equilibrium isotherm and ZLC response curves simulated under equilibrium control conditions. Type I isotherm. (C) Adsorption-Desorption equilibrium isotherm and ZLC response curves simulated under equilibrium control conditions. Type IV isotherm.

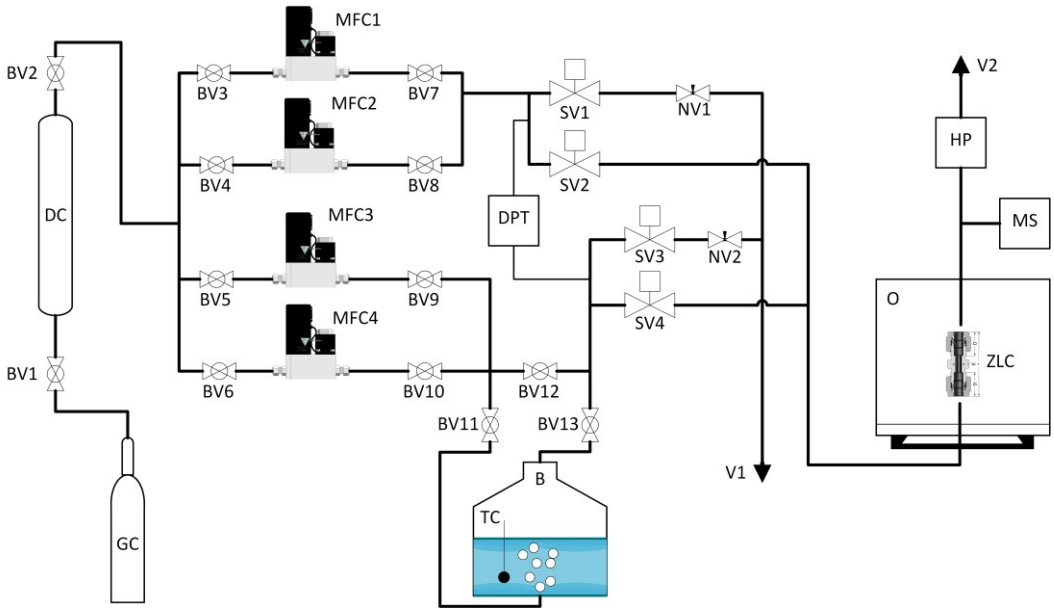

Fig. 2. Schematic flowsheet and components of the experimental ZLC system. GC carrier gas cylinder; DC drying column; BV ball valve; NV needle valve; TC water bath temperature controller; MFC mass flow controllers; B water bath; SV solenoid switching valve; V vent; O ZLC oven; ZLC zero length column; DPT differential pressure transducer; HP humidity probe; MS mass spectrometer.

682

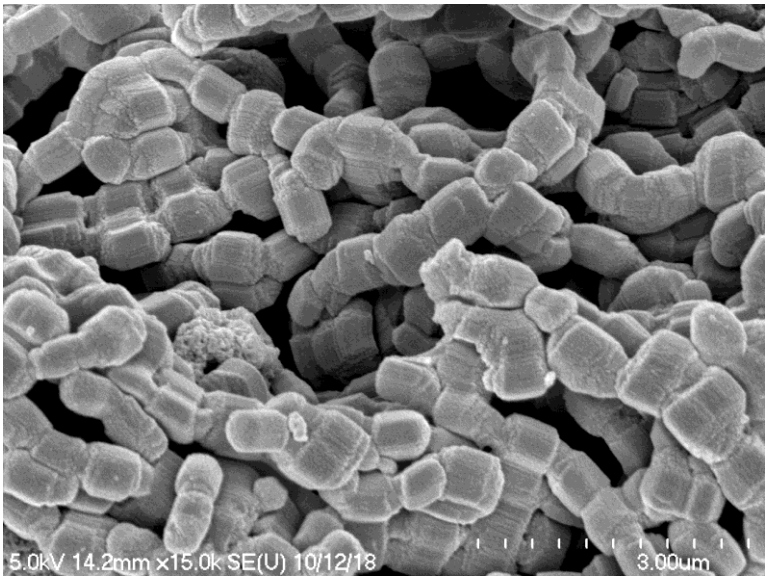

683

684

685

686

687 **Fig. 3.** SEM image of SBA-15 sample used in this study.

688

689

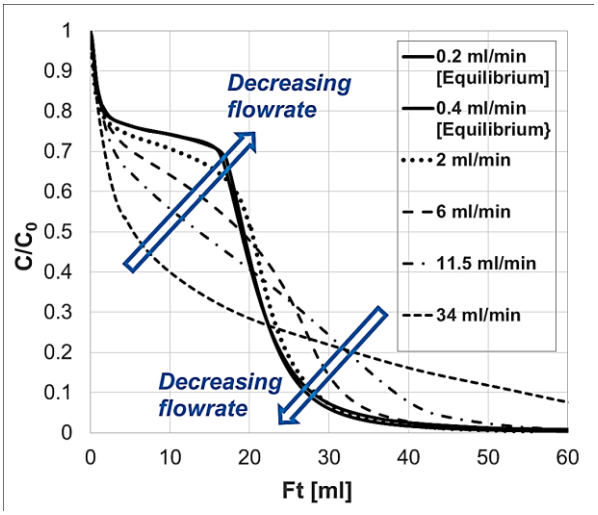

690

691

692

693

694 **Fig. 4.** Experimental *Ft-plot* for the evaluation of the control regime. Sample mass 1.2 mg. Initial

695 relative humidity = 86 %, at 298K and atmospheric pressure.

696

697

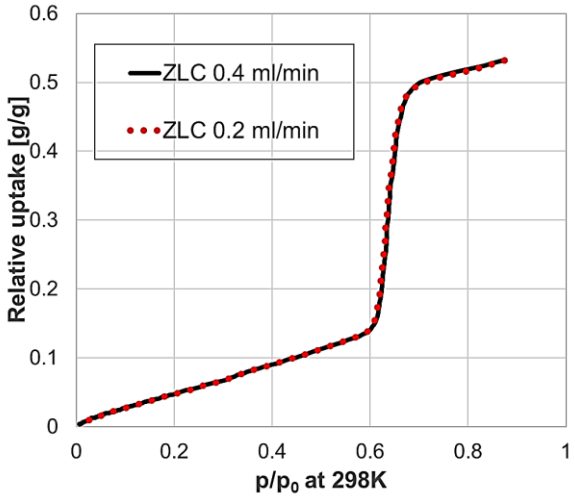

698

699

700

701

702 **Fig. 5.** Desorption isotherm calculated by using the two lowest flowrates shown in Fig. 4. Sample

703 mass 1.2 mg. Initial relative humidity = 86 % at 298K and atmospheric pressure.

704

705

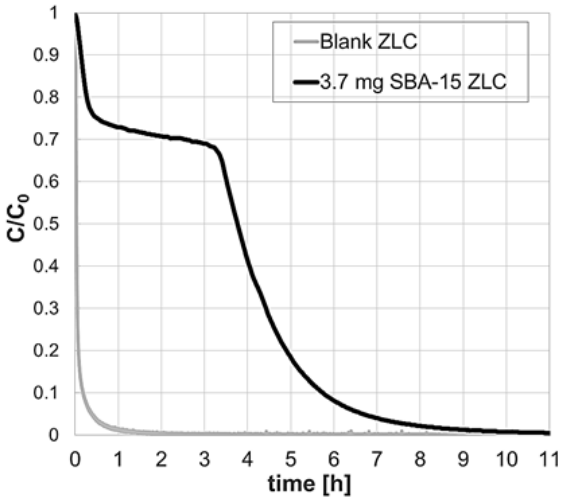

706

707

708

709 **Fig. 6.** Experimental response curves for the blank column and packed column. Sample mass 3.7

710 mg. Initial relative humidity = 86 % at 298K and atmospheric pressure.

711

712

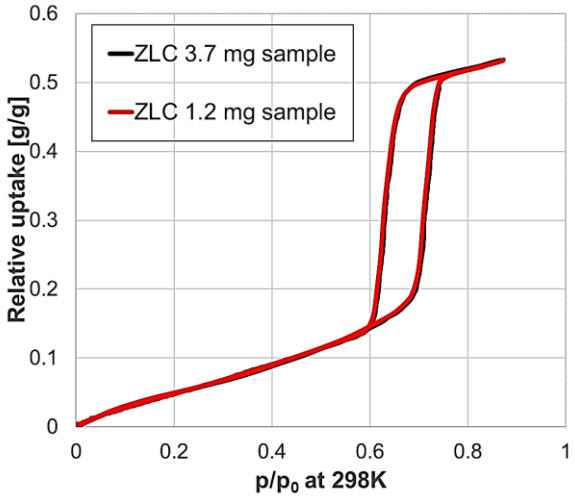

Fig. 7. Adsorption and desorption isotherms measured using two different sample masses. Initial relative humidity = 86 % and atmospheric pressure.

721

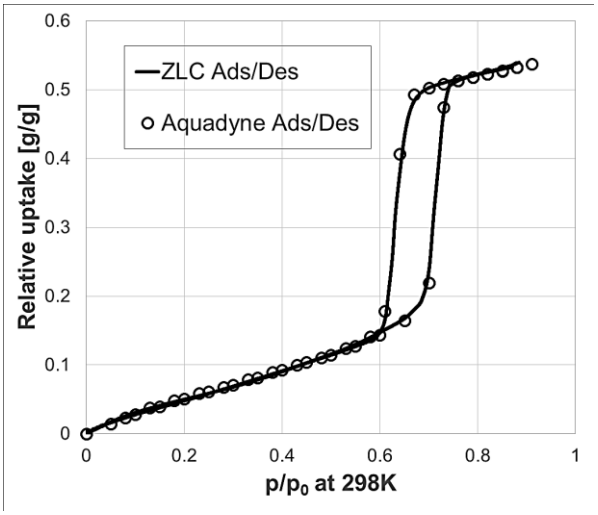

722

723

724

725

726 **Fig. 8.** Comparison between the isotherms measured with the ZLC system and gravimetric system.
727 ZLC sample mass 3.7 mg. Gravimetric sample mass 7 mg. Initial relative humidity = 86 % and
728 atmospheric pressure. Experimental signals are shown in Fig. 9.

729

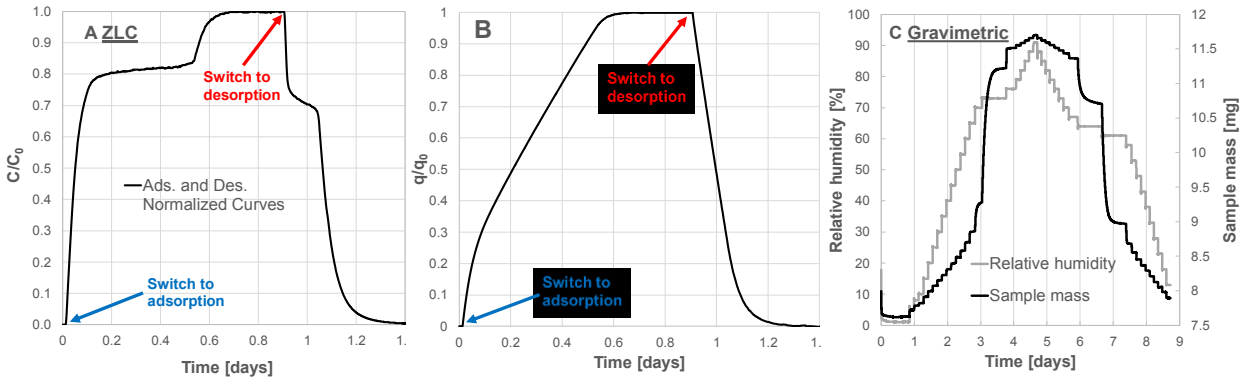

Fig. 9. (A) Experimental adsorption-desorption normalized response curves measured under equilibrium control conditions on the ZLC. (B) Adsorbed phase concentration vs time obtained from ZLC mass balance. Sample mass 3.7 mg. Highest relative humidity = 86 % at 298K and atmospheric pressure. (C) Experimental uptake curves obtained from the measurement of the equilibrium adsorption-desorption isotherm on the gravimetric system. Sample mass 7 mg.

741

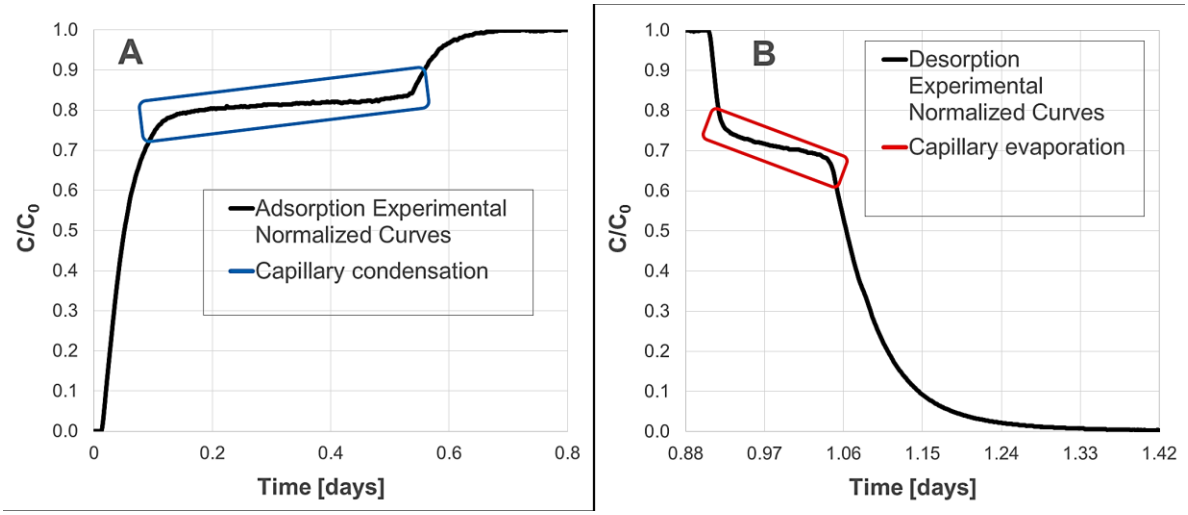

742

743

744

745 **Fig. 10.** Experimental normalized response curves measured under equilibrium control conditions
746 on the ZLC at 298K and atmospheric pressure. Sample mass 3.7 mg. (A) Measurement of the main
747 adsorption branch. Final relative humidity = 86 %. (B) Measurement of the main desorption
748 branch. Initial relative humidity = 86 %.

749

750

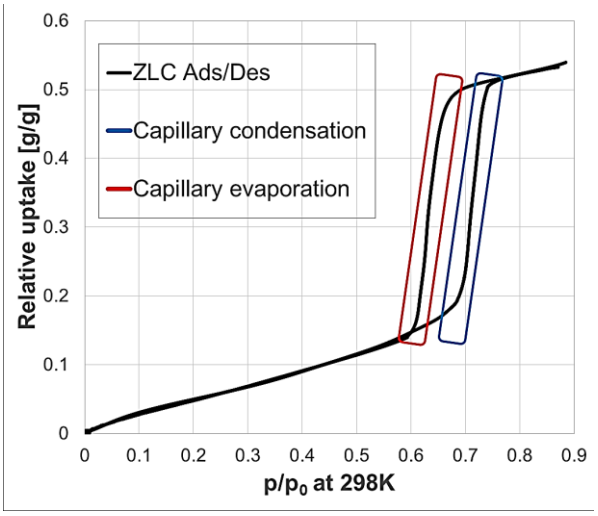

751

752

753

754

755 **Fig. 11.** Experimental adsorption-desorption isotherm calculated from the ZLC response curves
756 shown in Fig. 10. Sample mass 3.7 mg. Highest relative humidity = 86 % at 298K and atmospheric
757 pressure.

758

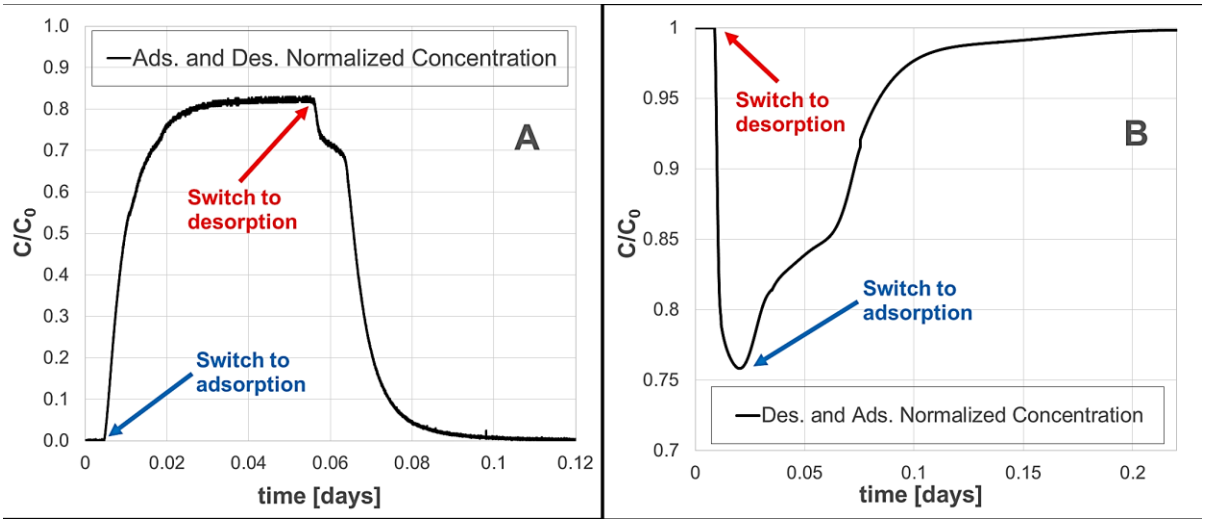

Fig. 12. Experimental adsorption-desorption normalized response curve measured under equilibrium control conditions at 298K and atmospheric pressure for sample mass 3.7 mg. (A) Measurement of the desorption scanning curve, t_{switch} = 12110 s. Initial relative humidity = 71.5 %. (B) Measurement of the adsorption scanning curve, t_{switch} = 1710 s. Initial relative humidity = 64 %.

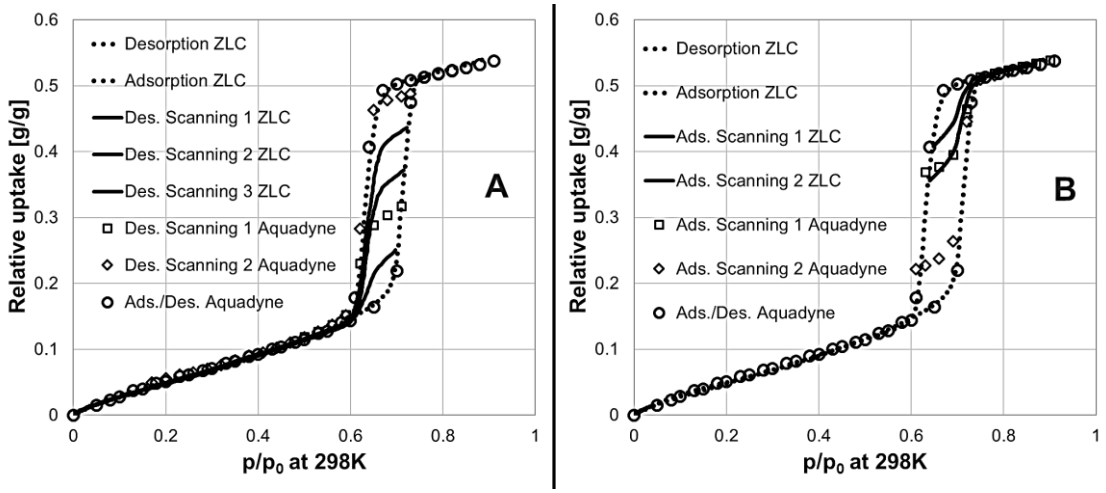

Fig. 13. (A) Desorption scanning curves measured on the ZLC system and gravimetric system. Initial relative humidity = 72.2 %, 71.5 % and, 69.7 %. ZLC sample mass 3.7 mg. Gravimetric sample mass 7 mg. (B) Adsorption scanning curves measured on the ZLC system and gravimetric system. Initial relative humidity = 64 % and, 64.8 %. ZLC sample mass 3.7 mg at 298K and atmospheric pressure. Gravimetric sample mass 7 mg.